

D²ST-Adapter: Disentangled-and-Deformable Spatio-Temporal Adapter for Few-shot Action Recognition

Wenjie Pei^{1,*}Qizhong Tan^{1,*}Guangming Lu¹Jiandong Tian²¹Harbin Institute of Technology, Shenzhen²Shenyang Institute of Automation, Chinese Academy of Sciences

wenjiecoder@outlook.com, 200110929@stu.hit.edu.cn, luguangm@hit.edu.cn, tianjd@sia.cn

Abstract

Adapting large pre-trained image models to few-shot action recognition has proven to be an effective and efficient strategy for learning robust feature extractors, which is essential for few-shot learning. Typical fine-tuning based adaptation paradigm is prone to overfitting in the few-shot learning scenarios and offers little modeling flexibility for learning temporal features in video data. In this work we present the Disentangled-and-Deformable Spatio-Temporal Adapter (D²ST-Adapter), a novel adapter tuning framework for few-shot action recognition, which is designed in a dual-pathway architecture to encode spatial and temporal features in a disentangled manner. Furthermore, we devise the Deformable Spatio-Temporal Attention module as the core component of D²ST-Adapter, which can be tailored to model both spatial and temporal features in corresponding pathways, allowing our D²ST-Adapter to encode features in a global view in 3D spatio-temporal space while maintaining a lightweight design. Extensive experiments with instantiations of our method on both pre-trained ResNet and ViT demonstrate the superiority of our method over state-of-the-art methods for few-shot action recognition. Our method is particularly well-suited to challenging scenarios where temporal dynamics are critical for action recognition.

1. Introduction

Few-shot action recognition aims to learn an action recognition model from a set of base classes of video data, which has the capability to recognize novel categories of actions using only a few support samples. To this end, learning an effective feature extractor that is generalizable across different classes is crucial to the task. A typical way [1, 2, 40, 41, 52] is to leverage pre-trained large vision models [13, 27, 35] for feature learning by task adaptation.

Most existing methods [26, 41, 42] seek to adapt large

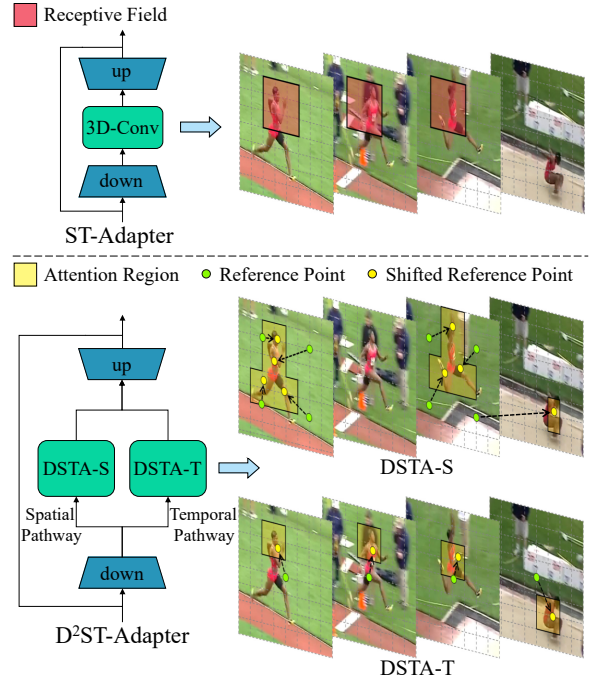


Figure 1. Different from ST-Adapter [25], our D²ST-Adapter is designed in a dual-pathway architecture to encode spatial and temporal features in a disentangled manner. Furthermore, we propose the Deformable Spatio-Temporal Attention (DSTA) as the essential component, which configures different sampling density in the spatial and temporal domains to model two pathways specifically and enables D²ST-Adapter to perform feature adaptation in a global view in 3D spatio-temporal space while maintaining a lightweight design.

vision models to few-shot action recognition by fine-tuning either the entire or partial model. While such methods have achieved promising performance, there are two important limitations that hamper them from exploiting the full potential of the pre-trained models. First, fully fine-tuning the pre-trained models is prone to overfitting in the few-shot learning scenarios whilst partial fine-tuning acquires limited effectiveness due to limited capacity for adaptation. Second, most large vision models are trained on im-

*Equal contribution.

Code is available at <https://github.com/qizhongtan/D2ST-Adapter>.

age data due to the difficulty of collecting a large scale of video data. Thus, these fine-tuning based methods require to learn the temporal features as a post-process after feature learning by the pre-trained backbone, typically by constructing an auxiliary module to model the temporal dynamics [34, 40, 42, 44], which has limited effectiveness compared to the learning manner throughout the whole feature encoding stage.

As a prominent parameter-efficient fine-tuning technique [12, 14, 17, 56], adapter tuning [4, 14, 39] embeds learnable adapters with a negligible amount of parameters into pre-trained models flexibly while keeping the model frozen, conducting task adaptation efficiently and effectively. ST-Adapter [25] makes the first attempt to apply adapter tuning to image-to-video transfer learning. As shown in Figure 1, it follows the classical bottleneck structure for adapter design [14] and inserts a 3D convolution layer in the bottleneck for feature transformation. Such a simple design can learn spatio-temporal features while maintaining a lightweight structure. Nevertheless, we investigate two potential limitations of ST-Adapter. First, it learns the spatial and temporal features jointly by 3D convolution, whereas it has been shown that such a joint learning paradigm of spatio-temporal features for video data is inferior to learning the spatial and temporal features in a disentangled way, such as SlowFast [8] or two-stream design [29, 38]. Second, the convolutional operation, especially with shallow layers for lightweight design, has a limited local receptive field in both the spatial and temporal domains, which also limits the performance of ST-Adapter.

In this work we design the Disentangled-and-Deformable Spatio-Temporal Adapter ($D^2ST\text{-Adapter}$) to tackle the limitations of ST-Adapter. Specifically, we design our $D^2ST\text{-Adapter}$ as a dual-pathway architecture, as illustrated in Figure 1, in which the spatial pathway is responsible for capturing the spatial appearance features while the temporal pathway focuses on learning the temporal dynamics. Thus, our model can encode the spatio-temporal features in a disentangled manner. Moreover, we devise the Deformable Spatio-Temporal Attention (DSTA) module as an essential component to model both the spatial and temporal pathways. It adapts the deformable attention [46] from 2D image space to 3D spatio-temporal space, which first samples a group of reference points in the spatio-temporal space and then learns the offset for each point to shift them to more informative regions in the 3D space. These shifted points are used as key and value pairs for DSTA to perform sparse self-attention, which allows our $D^2ST\text{-Adapter}$ to perform feature adaptation in a global view while maintaining a lightweight design.

A novel design of our DSTA is that we make the sampling density along the spatial and temporal domains configurable, which allows for tailoring specialized versions of

DSTA to model the spatial and temporal pathways separately. In particular, we tailor DSTA-T with denser sampling along the temporal domain than the spatial domain for the temporal pathway since it focuses on capturing temporal features. In contrast, the tailored DSTA-S for the spatial pathway samples denser reference points along the spatial domain. To conclude, we make the following contributions:

- We propose $D^2ST\text{-Adapter}$, a novel adapter tuning framework for few-shot action recognition, which is designed in a dual-pathway architecture to encode the spatial and temporal features in a disentangled manner.
- We devise the Deformable Spatio-Temporal Attention (DSTA), which can be tailored to model both the spatial and temporal pathways, allowing our $D^2ST\text{-Adapter}$ to encode features in a global view while maintaining a lightweight design.
- Extensive experiments on five standard benchmarks with instantiations of our method on pre-trained ResNet [13] and ViT [27], demonstrate the superiority of our method over other state-of-the-art methods, particularly in challenging scenarios like the SSv2 benchmark where the temporal dynamics are critical for action recognition. Besides, comprehensive ablation study is conducted to investigate our $D^2ST\text{-Adapter}$ thoroughly.

2. Related Work

Few-shot image classification. Existing works for few-shot image classification can be categorized into three groups: augmentation-based, optimization-based, and metric-based. Augmentation-based methods mainly hallucinate [11, 43] and generate [20, 53] new training samples adversarially to prevent the model from over-fitting. Optimization-based algorithms [9, 16, 28] aim to train a model that generalizes well and can be quickly adapted to new tasks through a few gradient update steps. Metric-based approaches recognize novel samples through nearest neighbor classification using a specific distance metric, such as cosine similarity [37, 50], Euclidean distance [6, 30, 51], and learnable metrics [32]. Our work follows the metric-based category due to its simplicity and effectiveness, and we focus on the more challenging video setting.

Few-shot action recognition. Most existing few-shot action recognition methods adopt the metric-based paradigm to classify videos, and primarily focus on two directions to deal with this task. The first one is to investigate the spatio-temporal modeling [34, 42, 44, 45, 48, 52, 54, 57, 58]. For example, MTFAN [44] proposes a motion encoder to learn global motion patterns and injects them into each video representations using a motion modulator. STRM [34] enriches local patch features and global frame features for joint spatio-temporal modeling. MoLo [42] designs a motion auto-decoder to explicitly extract motion dynamics in a unified network. Our method also aims to model spatio-temporal

features effectively and efficiently based on adapter-tuning technique. Another direction focuses on designing effective metric learning strategy [1, 2, 15, 24, 26, 40, 44, 55]. OTAM [2] utilizes the DTW [23] algorithm to calculate video distances with strict temporal alignment. TRX [26] exhaustively enumerates all sub-sequences of support and query videos and matches them using an attention mechanism. HyRSM [40] applies a novel bidirectional mean Hausdorff metric (referred to as Bi-MHM) to alleviate the strictly ordered constraints. We evaluate our D^2ST -Adapter using the above three classical matching strategies to demonstrate its effectiveness and robustness.

Adapter tuning. As a classical parameter-efficient fine-tuning method, adapter tuning method is first proposed in [14], and quickly draws attention in many other research areas [4, 12, 33, 39]. A common practice is to build up a lightweight module (named *Adapter*) which only consisting of negligible learnable parameters, and selectively plug it into a pre-trained model. During training, only the parameters of inserted adapters are updated while the original model remains frozen, leading to efficient task adaptation. Recently, some works apply this method to adapt image models for video recognition. AIM [49] inserts adapters into different parts of each ViT [7] stage for spatial, temporal, and joint adaptation, separately. ST-Adapter [25] employs depth-wise 3D convolution to construct adapter for feature adaptation, which endows it with spatio-temporal modeling capability. Our D^2ST -Adapter follows the basic framework of ST-Adapter, and meanwhile optimize the essential technical designs for few-shot action recognition.

3. Method

3.1. Overview

Problem Formulation. The aim of few-shot action recognition is to learn an action recognizer from a set of base classes, which is able to recognize novel classes using only a few labeled samples. The task typically follows episodic paradigm [2, 37, 40, 42], which is consistent with general application scenarios for few-shot learning. An episode includes a support set \mathcal{S} consisting of N classes and K labeled samples for each class (referred to as the N -way K -shot task), as well as a query set \mathcal{Q} that contains unlabeled samples to be classified. In each episode, we aim to classify every query into one of the N classes with the guidance of the support set. Such episodic task setting is consistently adopted during all the training, validation, and test stages.

Adapter Tuning Framework. We design a plug-and-play and lightweight adapter, dubbed D^2ST -Adapter, which can be integrated into most of existing deep feature learning framework of vision models. Thus we can leverage the powerful feature encoding capability of pre-trained large vision models by adapting them into the task of few-shot action recognition efficiently while incurring only a small

amount of parameter-tuning overhead.

Figure 2 (a) illustrates the overall adapter tuning framework of our method. Given a pre-trained feature extractor from a large model, our designed lightweight D^2ST -Adapter can be selectively plugged into the middle layers of the feature extractor to perform feature transformation for task adaptation while maintaining the shape of feature maps consistent before and after each adaptation. Only the inserted adapters are tuned during training while the pre-trained backbone keeps frozen, leading to efficient task adaptation. The learned features by such adapter tuning framework are further used for few-shot action recognition based on the metric-based strategy [2, 30, 42].

Our D^2ST -Adapter is designed independently from the backbone structure of the feature extractor, thus it can be readily integrated into most of classical pre-trained deep vision models. In particular, we instantiate the backbone of feature extractor with two dominant deep visual learning frameworks, namely ResNet [13] and ViT [7], respectively.

3.2. D^2ST -Adapter

Dual-pathway Adapter Architecture for Spatio-Temporal Disentanglement. Successful action recognition from video data entails effective feature learning of both spatial semantic and temporal dynamic features. Most large vision models are typically pre-trained on image data, thus our D^2ST -Adapter should be capable of capturing both the spatial features and temporal features. To this end, we design the D^2ST -Adapter as a dual-pathway architecture shown in Figure 2 (c), in which the spatial pathway is responsible for capturing the spatial semantics while the temporal pathway focuses on learning the temporal dynamics. As a result, our model is able to encode the spatio-temporal features for video data in a disentangled manner.

As a common practice of typical Adapters [14, 25], our D^2ST -Adapter adopts the bottleneck architecture for reducing the computational complexity. It first downsamples the feature map into a low-dimensional feature space, then the downsampled features are fed into the spatial and temporal pathways concurrently to perform disentangled feature adaptation. Finally, both the adapted spatial and temporal features are fused by simple element-wise addition and upsampled back to the initial size. Formally, given the feature maps $\mathbf{F}_i^{\text{in}} \in \mathbb{R}^{T \times H \times W \times C}$ obtained from the i -th stage of the pre-trained backbone, containing C channels of feature maps with spatial size $H \times W$ for each of T frames, the feature adaptation by D^2ST -Adapter can be formulated as:

$$\mathbf{F}_i^{\text{out}} = \text{GELU}(\mathcal{F}_S(\mathbf{F}_i^{\text{in}} \cdot \mathbf{W}_{\text{down}}) \oplus \mathcal{F}_T(\mathbf{F}_i^{\text{in}} \cdot \mathbf{W}_{\text{down}})) \cdot \mathbf{W}_{\text{up}}. \quad (1)$$

Herein, $\mathbf{W}_{\text{down}} \in \mathbb{R}^{C \times C'}$ and $\mathbf{W}_{\text{up}} \in \mathbb{R}^{C' \times C}$ are the transformation matrices of two linear layers for downsampling and upsampling, respectively. \mathcal{F}_S and \mathcal{F}_T denote the disen-

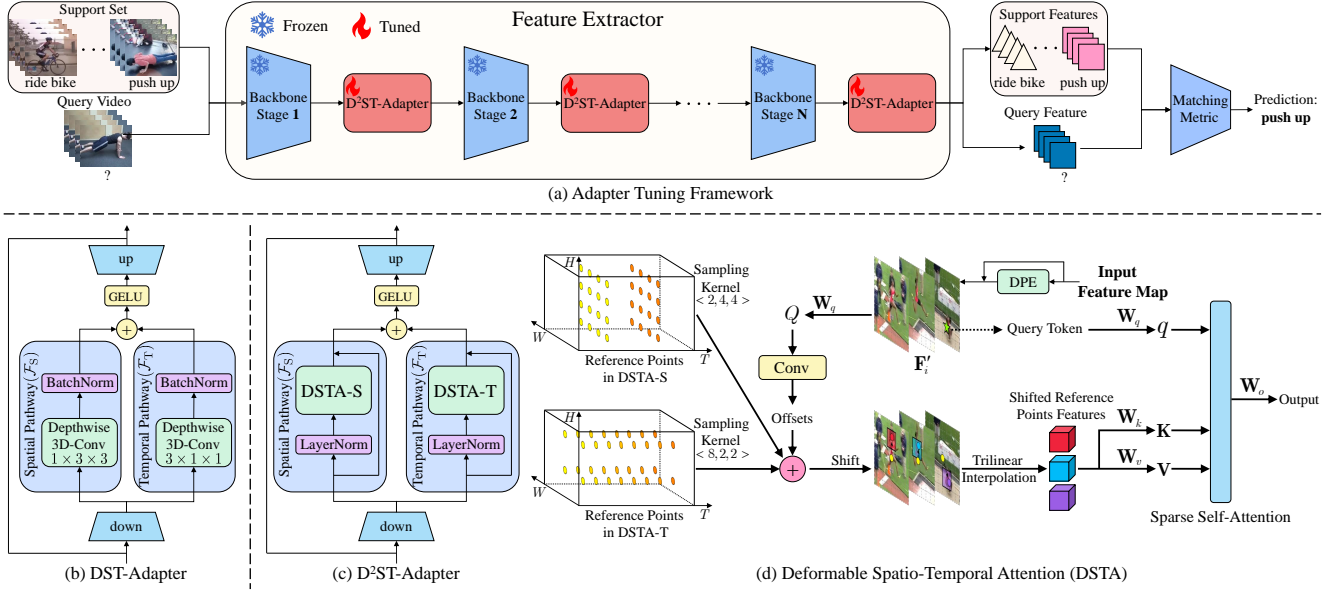


Figure 2. (a) Overall adapter tuning framework of our method. (b) DST-Adapter, a convolutional version of our model, which also follows dual-pathway architecture, whereas both pathways are constructed based on 3D convolution. (c) D²ST-Adapter, which is designed in a dual-pathway architecture and both pathways are modeled based on the proposed DSTA illustrated in (d).

tangled feature adaptation by the spatial and temporal pathways respectively. Below we discuss two feasible modeling mechanisms for \mathcal{F}_S and \mathcal{F}_T , which leverages 3D convolution and our proposed Deformable Spatio-Temporal Attention, respectively.

Modeling with 3D Convolution. A straightforward way to model the disentangled spatio-temporal feature adaptation (\mathcal{F}_S and \mathcal{F}_T in Equation 1) is to employ 3D convolutional network, which can be tailored by configuring the shape of convolutional kernels to focus on learning either the spatial or the temporal features. Specifically, we model both \mathcal{F}_S and \mathcal{F}_T using 3D depth-wise convolutional layers followed by a batch normalization layer and a GELU layer, as shown in Figure 2 (b). The only difference between the modeling of them is that \mathcal{F}_S uses $1 \times 3 \times 3$ convolutional kernel for capturing spatial features while \mathcal{F}_T is constructed with $3 \times 1 \times 1$ convolutional layer to learn the temporal dynamics. The resulting version is called *DST-Adapter*.

While it has been validated that leveraging 3D convolutions with different kernel shapes can learn the spatial and temporal features separately [8, 36], An important limitation of using 3D convolutions to construct *D²ST-Adapter*, which is also suffered by *ST-Adapter*, is that the convolutional operation has limited local receptive field either in the spatial or the temporal domain. Constructing deep convolutional network by stacking convolutional layers can enlarge the receptive field whilst increasing the model size and incurring heavy computational burden, which is inconsistent with the lightweight design principle for adapters.

Modeling with Deformable Spatio-Temporal Attention. To address the limitation of the modeling mechanism based

on 3D convolution (DST-Adapter), we devise Deformable Spatio-Temporal Attention (DSTA) which performs feature adaptation in a global view by sparse self-attention while maintaining high computational efficiency. It adapts the deformable attention [46] from 2D image space to 3D spatio-temporal space. As shown in Figure 2 (d), similar to the deformable attention, DSTA first samples a group of reference points in the spatio-temporal space and then learns the offset for each reference point to shift them to the more informative regions. As a result, DSTA can learn a set of informative tokens which are further used as key and value pairs shared for all queries for sparse self-attention.

We conduct several adaptations from the deformable attention in 2D space to our DSTA in spatio-temporal 3D space. First, we employ Dynamic Position Embedding (DPE) [21] implemented as a 3D depth-wise convolution layer to learn the semantic-conditioned spatio-temporal position information for each token and incorporate it into the semantic features by simple element-wise addition. Thus, the feature map $\mathbf{F}'_i \in \mathbb{R}^{T \times H \times W \times C'}$ fused with the position information at the i -th stage is obtained by:

$$\mathbf{F}'_i = \mathcal{F}_{\text{DPE}}(\mathbf{F}_i^{\text{in}} \cdot \mathbf{W}_{\text{down}}) \oplus (\mathbf{F}_i^{\text{in}} \cdot \mathbf{W}_{\text{down}}). \quad (2)$$

Our DSTA learns the offsets in 3D space for the reference points by a 3D convolutional network consisting of a 3D depth-wise convolution layer and a $1 \times 1 \times 1$ 3D convolution layer as well as a GELU in between. After shifting the reference points according to the learned offsets, we derive the features for each shifted reference point by performing trilinear interpolation among neighboring tokens within a 3D volume space around the point. For instance, the features

for the shifted point \mathbf{p} located at (p_t, p_h, p_w) is calculated via the trilinear interpolation $\mathcal{F}_{\text{tri-int}}$ by:

$$\mathcal{F}_{\text{tri-int}}(\mathbf{p}) = \sum_{\mathbf{r}} g(p_t, r_t) \cdot g(p_h, r_h) \cdot g(p_w, r_w) \cdot \mathbf{F}'_i(\mathbf{r}), \quad (3)$$

where $g(a, b) = \max(0, 1 - |a - b|)$ defines the interpolating volume space and $\mathbf{r} = (r_t, r_h, r_w)$ indexes all token in the whole spatio-temporal 3D space. All shifted reference points are used as the keys and values shared for sparse self-attention. For instance, a token in \mathbf{F}'_i located at (u_t, u_h, u_w) serves as a query and the output $\mathbf{Z}'_{i,(u_t,u_h,u_w)}$ of DSTA is calculated by:

$$\begin{aligned} \mathbf{q} &= \mathbf{F}'_{i,(u_t,u_h,u_w)} \cdot \mathbf{W}_q, \mathbf{K} = \mathbf{P} \cdot \mathbf{W}_k, \mathbf{V} = \mathbf{P} \cdot \mathbf{W}_v, \\ \mathbf{Z}'_{i,(u_t,u_h,u_w)} &= \text{softmax}(\mathbf{q}\mathbf{K}/\sqrt{C'})\mathbf{V} \cdot \mathbf{W}_o, \end{aligned} \quad (4)$$

where $\mathbf{P} \in \mathbb{R}^{M \times C'}$ is the stacked feature matrix of all M shifted points and $\mathbf{W}_q, \mathbf{W}_k, \mathbf{W}_v, \mathbf{W}_o$ are projection matrices for the query, key, value and output respectively.

The learned offsets for reference points is restricted in a limited range for two reasons. First, it can prevent the potential training collapse that all reference points are shifted to the same point. Second, such restriction can ensure that each reference point can be shifted to a unique location within a local region. As a result, more sampling of reference points typically lead to more powerful and fine-grained representation by the shifted points. The deformable attention samples reference points uniformly in the 2D feature space with the same sampling density along two spatial dimensions. In contrast, we make the sampling density in the spatial and temporal domains configurable. Consequently, our $D^2ST\text{-Adapter}$ can leverage DSTA to model both \mathcal{F}_S in the spatial pathway for spatial feature adaptation and \mathcal{F}_T in the temporal pathway for temporal feature adaptation. Specifically, we define the ‘*Sampling kernel*’ for DSTA as:

Definition 1. *Sampling kernel*: formulated as the sampling densities of reference points along the dimensions of time, height and width, respectively, denoted as $\langle n_t, n_s, n_s \rangle$, s.t. $M = n_t \times n_s \times n_s$. Herein, M is the total number of sampled reference points.

Intuitively, a DSTA module whose sampling kernel has large n_t and small n_s are more capable of learning the temporal features than learning the spatial features. On the other hand, sampling more reference points in the spatial domain than the temporal domain ($n_s > n_t$) generally makes DSTA focus on learning the spatial features. Thus, we can tailor DSTA by configuring the sampling kernel to model \mathcal{F}_S and \mathcal{F}_T correspondingly. In particular, we tailor two versions of DSTA:

- **DSTA-S** for modeling \mathcal{F}_S in the spatial pathway, whose sampling kernel has relatively large n_s and small n_t ($n_s > n_t$).
- **DSTA-T** for modeling \mathcal{F}_T in the temporal pathway, which samples denser reference points in the temporal domain than in the spatial domain ($n_t > n_s$).

In practice, the values of n_t and n_s are tuned as hyper-parameters. Such modeling is analogous to classical property of 3D convolutional network that configuring the shape of the convolutional kernel can steer the convolutional operation to focus on learning features in different domain.

3.3. End-to-End Adapter Tuning

The learned features by our adapter tuning framework are further used for few-shot action recognition based on the metric-based strategy. It first calculates the frame-wise L_2 distance matrix between the input query video and each class prototype derived by simply averaging the corresponding support samples. Then the distance matrix is used to calculate the matching similarity between the query and each class for prediction. The whole model can be optimized in an end-to-end manner using the cross-entropy loss.

4. Experiments

4.1. Experimental Setup

Datasets. We conduct experiments on five standard few-shot action recognition benchmarks, including SSv2-Full [10], SSv2-Small [10], Kinetics [3], HMDB51 [19], and UCF101 [31]. The temporal features are crucial to the action recognition in SSv2-Full and SSv2-Small while the actions in other datasets relies more on the spatial features than the dynamic features. Following the typical data split [2, 42, 57], For SSv2-Full, SSv2-Small and Kinetics, we select 64/24/12 classes from the datasets as the training/validation/test set, respectively. As for HMDB51 and UCF101, we adopt the same data split as [42, 52].

Pre-trained backbone. Most prior arts employs the ResNet-50 [13] pre-trained on ImageNet [5] as backbone to extract frame features. Recently, CLIP-FSAR [41] conduct experiments on CLIP-ViT-B [7] and get remarkable performance. To verify the effectiveness of our $D^2ST\text{-Adapter}$, we instantiate our method with both pre-trained backbones.

Implementation details. We insert one $D^2ST\text{-Adapter}$ module in each stage of the pre-trained model (4 stages for ResNet-50 and 12 stages for CLIP-ViT-B) as shown in Figure 2 (a). We tune the sampling kernel for DSTA-S and DSTA-T for each backbone and the details are provided in the supplementary material. For a fair comparison with previous methods [2, 40, 42], we uniformly sample 8 frames (i.e., $T = 8$) as the input of a video. We employ several standard techniques for data augmentation such as random crop and color jitter in the training stage. Bi-MHM [40] is used as the matching metric in comparison with other methods. Besides, OTAM [2] and TRX [26] are additionally used in the ablation study. We train the model episodically with Adam [18] optimizer. Following the common practice [40, 42], in the test stage, we randomly select 10,000 episodes from the test set and report the average accuracy.

Table 1. Classification accuracy (%) of different methods on SSv2-Full and SSv2-Small that are challenging benchmarks where both the temporal and spatial features are crucial to action recognition. The highest and the second best results of both backbones are highlighted in **bold** and underline, respectively.

Method	Reference	Backbone	Adaptation paradigm	SSv2-Full					SSv2-Small		
				1-shot	2-shot	3-shot	4-shot	5-shot	1-shot	3-shot	5-shot
CMN [57]	ECCV(18)	ResNet-50	Full fine-tuning	34.4	—	—	—	43.8	33.4	42.5	46.5
CMN-J [58]	TPAMI(20)	ResNet-50	Full fine-tuning	—	—	—	—	—	36.2	44.6	48.8
OTAM [2]	CVPR(20)	ResNet-50	Full fine-tuning	42.8	49.1	51.5	52.0	52.3	36.4	45.9	48.0
ITANet [54]	IJCAI(21)	ResNet-50	Full fine-tuning	49.2	55.5	59.1	61.0	62.3	39.8	49.4	53.7
TRX [26]	CVPR(21)	ResNet-50	Full fine-tuning	42.0	53.1	57.6	61.1	64.6	36.0	51.9	59.1
TA ² N [22]	AAAI(22)	ResNet-50	Full fine-tuning	47.6	—	—	—	61.0	—	—	—
MTFAN [44]	CVPR(22)	ResNet-50	Full fine-tuning	45.7	—	—	—	60.4	—	—	—
STRM [34]	CVPR(22)	ResNet-50	Full fine-tuning	43.1	53.3	59.1	61.7	68.1	37.1	49.2	55.3
HyRSM [40]	CVPR(22)	ResNet-50	Full fine-tuning	54.3	62.2	65.1	67.9	69.0	40.6	52.3	56.1
Nguyen <i>et al.</i> [24]	ECCV(22)	ResNet-50	Full fine-tuning	43.8	—	—	—	61.1	—	—	—
Huang <i>et al.</i> [15]	ECCV(22)	ResNet-50	Full fine-tuning	49.3	—	—	—	66.7	38.9	—	61.6
HCL [55]	ECCV(22)	ResNet-50	Full fine-tuning	47.3	54.5	59.0	62.4	64.9	38.7	49.1	55.4
SloshNet [47]	AAAI(23)	ResNet-50	Full fine-tuning	46.5	—	—	—	68.3	—	—	—
GgHM [48]	ICCV(23)	ResNet-50	Full fine-tuning	54.5	—	—	—	69.2	—	—	—
MoLo [42]	CVPR(23)	ResNet-50	Full fine-tuning	56.6	62.3	67.0	68.5	70.6	42.7	52.9	56.4
ST-Adapter [25]	NeurIPS(22)	ResNet-50	Adapter tuning	52.2	59.9	64.1	67.1	68.7	41.9	51.5	55.7
D²ST-Adapter (Ours)	—	ResNet-50	Adapter tuning	57.0	65.2	69.5	71.4	73.6	45.8	56.6	60.9
CLIP-FSAR [41]	ArXiv(23)	CLIP-ViT-B	Full fine-tuning	61.9	64.9	68.1	70.9	72.1	<u>54.5</u>	58.6	61.8
ST-Adapter [25]	NeurIPS(22)	CLIP-ViT-B	Adapter tuning	<u>64.2</u>	<u>72.4</u>	<u>76.0</u>	<u>77.4</u>	<u>79.5</u>	53.1	<u>64.2</u>	<u>68.0</u>
D²ST-Adapter (Ours)	—	CLIP-ViT-B	Adapter tuning	66.7	75.3	78.3	80.1	81.9	55.0	65.8	69.3

4.2. Comparison with State-of-the-Art Methods

Benchmarks sensitive to temporal features. Table 1 shows the comparative results of different methods on SSv2-Full and SSv2-Small, which are quite challenging since both the temporal and spatial features are crucial to the action recognition. Our *D²ST-Adapter* achieves the best performance and outperforms other methods by a large margin with both backbones in all few-shot settings except ‘5-shot’ on SSv2-Small. These results demonstrate the advantages of our method over other methods in dealing with challenging scenarios where the temporal features are critical for action recognition. In particular, our *D²ST-Adapter* outperforms ST-Adapter substantially on all settings, which reveals the benefit of two core technical designs of *D²ST-Adapter*, namely the dual-pathway architecture for disentangled learning of spatial and temporal features and Deformable Spatio-Temporal Attention for learning features in a global view.

To obtain more insight into the strength and weakness of our *D²ST-Adapter*, we select four categories of actions that our method excels at as well as four categories that our model struggles with at compared with the state-of-the-art MoLo and ST-Adapter. Figure 3 shows that our model achieves large performance superiority over other methods on the relatively complex actions requiring careful reasoning via learning temporal features for recognition, whilst performing poorly on simple actions that can be recognized primarily based on spatial features. Such results are consistent with the previous results that our model excels at recognizing actions involving complex temporal dynamics.

Benchmarks relying on spatial features. Table 2 presents the experimental results on the benchmarks relying more on

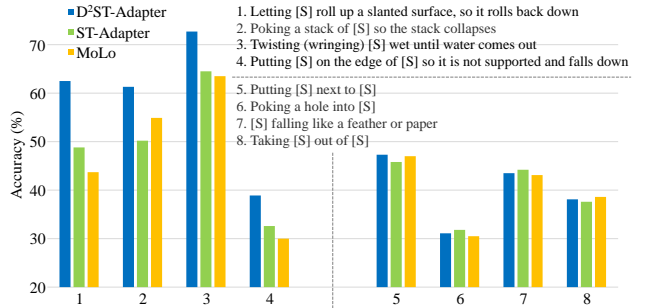


Figure 3. Illustration of actions our method excels at (1-4) and performs poorly at (5-8), respectively. The performance is evaluated on SSv2-Small benchmark in 1-shot setting.

spatial features, including Kinetics, HMDB51 and UCF101. Our method still performs best on most of the settings, which manifest the effectiveness and robustness of our method in these scenarios. We also observe that the performance improvement by our *D²ST-Adapter* over other method, especially ST-Adapter, is smaller than that on SSv2 datasets. It is reasonable since the action recognition in these datasets relies less on the temporal features and thus the disentangled feature encoding of our method yields limited performance gain.

Comparison of efficiency. We compare the efficiency between our *D²ST-Adapter* and other methods in terms of tunable parameter size and memory usage in Figure 4. It shows that the tunable parameter size of both our model and ST-Adapter is significantly smaller than other methods that are based on full fine-tuning for task adaptation, which reveals the advantage of the adapter tuning paradigm over the full fine-tuning paradigm for task adaptation. Meanwhile, our method outperforms these full fine-tuning based methods substantially while enjoying much fewer tunable param-

Table 2. Classification accuracy (%) of different methods on Kinetics, HMDB51 and UCF101 where spatial features are more crucial for action recognition. The highest and the second best results of both backbones are highlighted in **bold** and underline, respectively.

Method	Reference	Backbone	Adaptation paradigm	Kinetics					HMDB51			UCF101		
				1-shot	2-shot	3-shot	4-shot	5-shot	1-shot	3-shot	5-shot	1-shot	3-shot	5-shot
CMN [57]	ECCV(18)	ResNet-50	Full fine-tuning	57.3	67.5	72.5	74.7	76.0	—	—	—	—	—	—
CMN-J [58]	TPAMI(20)	ResNet-50	Full fine-tuning	60.5	70.0	75.6	77.3	78.9	—	—	—	—	—	—
OTAM [2]	CVPR(20)	ResNet-50	Full fine-tuning	73.0	75.9	78.7	81.9	85.8	54.5	65.7	68.0	79.9	87.0	88.9
ITANet [54]	IJCAI(21)	ResNet-50	Full fine-tuning	73.6	—	—	—	84.3	—	—	—	—	—	—
TRX [26]	CVPR(21)	ResNet-50	Full fine-tuning	63.6	76.2	81.8	83.4	85.9	53.1	66.8	75.6	78.2	92.4	96.1
TA ² N [22]	AAAI(22)	ResNet-50	Full fine-tuning	72.8	—	—	—	85.8	59.7	—	73.9	81.9	—	95.1
MTFAN [44]	CVPR(22)	ResNet-50	Full fine-tuning	74.6	—	—	—	87.4	59.0	—	74.6	84.8	—	95.1
STRM [34]	CVPR(22)	ResNet-50	Full fine-tuning	62.9	76.4	81.1	83.8	86.7	52.3	67.4	77.3	80.5	92.7	96.9
HyRSM [40]	CVPR(22)	ResNet-50	Full fine-tuning	73.7	80.0	83.5	84.6	86.1	60.3	71.7	76.0	83.9	93.0	94.7
Nguyen <i>et al.</i> [24]	ECCV(22)	ResNet-50	Full fine-tuning	74.3	—	—	—	87.4	59.6	—	76.9	84.9	—	95.9
Huang <i>et al.</i> [15]	ECCV(22)	ResNet-50	Full fine-tuning	73.3	—	—	—	86.4	60.1	—	77.0	71.4	—	91.0
HCL [55]	ECCV(22)	ResNet-50	Full fine-tuning	73.7	79.1	82.4	84.0	85.8	59.1	71.2	76.3	82.5	91.0	93.9
SloshNet [47]	AAAI(23)	ResNet-50	Full fine-tuning	70.4	—	—	—	87.0	59.4	—	77.5	<u>86.0</u>	—	97.1
GgHM [48]	ICCV(23)	ResNet-50	Full fine-tuning	<u>74.9</u>	—	—	—	87.4	<u>61.2</u>	—	76.9	85.2	—	96.3
MoLo [42]	CVPR(23)	ResNet-50	Full fine-tuning	74.0	<u>80.4</u>	<u>83.7</u>	<u>84.7</u>	85.6	60.8	<u>72.0</u>	<u>77.4</u>	<u>86.0</u>	<u>93.5</u>	95.5
ST-Adapter [25]	NeurIPS(22)	ResNet-50	Adapter tuning	73.0	79.9	82.8	84.6	85.1	60.3	71.4	74.7	84.6	92.9	94.5
D²ST-Adapter (Ours)	—	ResNet-50	Adapter tuning	75.0	81.4	84.3	85.8	87.0	61.6	73.0	76.6	86.9	94.4	95.6
CLIP-FSAR [41]	ArXiv(23)	CLIP-ViT-B	Full fine-tuning	89.7	92.9	94.2	94.8	95.0	75.8	84.1	87.7	96.6	98.4	99.0
ST-Adapter [25]	NeurIPS(22)	CLIP-ViT-B	Adapter tuning	88.5	92.6	94.0	94.6	95.1	74.1	<u>84.3</u>	87.3	95.9	<u>98.5</u>	98.9
D²ST-Adapter (Ours)	—	CLIP-ViT-B	Adapter tuning	<u>89.3</u>	93.1	94.4	95.2	95.5	77.1	86.4	88.2	<u>96.4</u>	98.7	99.1

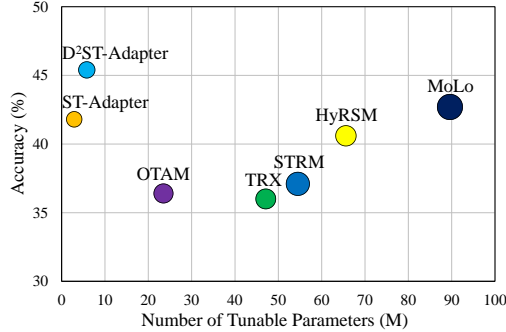


Figure 4. Performance and efficiency of different methods on SSV2-Small dataset in the 5-way 1-shot setting. Circle size indicates the memory usage during training.

ters, which validates the superiority of our method.

4.3. Ablation study

We conduct ablation study by using ResNet-50 as the pre-trained backbone and Bi-MHM [40] as the matching metric. **Comparison between different Adapters.** We first compare the performance of different Adapters in Table 3. Vanilla-Adapter is the initially proposed adapter [14] which only contains the downsampling and upsampling layers with a GELU nonlinearity in between. As described in Section 3.2, DST-Adapter is the convolutional version of our *D²ST-Adapter* which follows the dual-pathway structure but models spatial and temporal pathways with 3D convolution. The performance of full fine-tuning is also provided for reference. We make following observations.

- Effect of learning temporal features by adapters. ST-Adapter outperforms Vanilla-Adapter distinctly, which indicates that using 3D convolution to learn joint spatio-temporal features facilitates the feature adaptation.
- Effect of disentangled encoding of the spatial and temporal features. The performance improvement from ST-Adapter to DST-Adapter demonstrates the effectiveness of dual-pathway adapter architecture, which allows for

Table 3. Comparison between different adapters as well as full fine-tuning on SSV2-Full and Kinetics.

Method	SSv2-Full		Kinetics	
	1-shot	5-shot	1-shot	5-shot
Full Fine-tuning	44.9	57.0	72.4	84.3
Vanilla-Adapter	45.3	57.6	72.6	84.8
ST-Adapter	52.2	68.7	73.0	85.1
DST-Adapter (Ours)	53.7	69.6	73.3	85.5
D²ST-Adapter (Ours)	57.0	73.6	75.0	87.0

Table 4. Ablation study on the configuration of sampling kernel of DSTA on SSV2-Full and Kinetics datasets.

Configuration	SSv2-Full		Kinetics	
	1-shot	5-shot	1-shot	5-shot
DSTA-Uniform	55.8	72.2	73.9	86.0
DSTA-S & DSTA-T	57.0	73.6	75.0	87.0

encoding the spatial and temporal features in a disentangled manner.

- Effect of the proposed Deformable Spatial-Temporal Attention (DSTA). Comparing our *D²ST-Adapter* with DST-Adapter, the proposed DSTA yields a large performance gain, especially on the SSV2-Full dataset, which is more challenging due to the necessity of encoding temporal features.

Effect of configuration of the sampling kernel of DSTA.

To investigate the effect of configuring specialized sampling kernels for DSTA-S in the spatial pathway and DSTA-T in the temporal pathway respectively, we additionally configure a DSTA-Uniform module, which performs sampling with uniform density in both the spatial and temporal domains. Then we compare the performance of our *D²ST-Adapter* using two different settings, including 1) ‘DSTA-Uniform’, in which DSTA-Uniform is used to model both the spatial and temporal pathways and 2) ‘DSTA-S & DSTA-T’, in which *D²ST-Adapter* uses DSTA-S and DSTA-T to model the spatial and temporal pathways respectively. As shown in Table 4, the distinct performance gap between these two settings reveals the advantage of



Figure 5. Visualization of shifted reference points in both pathways for two video samples. Circle size indicates the importance for each point calculated by aggregating the attention from all queries.

Table 5. Evaluation of generalization of our D^2ST -Adapter across different matching metrics on SSv2-Full and Kinetics. The state-of-the-art methods for each metric are involved into comparison.

Matching Metric	Method	SSv2-Full		Kinetics	
		1-shot	5-shot	1-shot	5-shot
OTAM [2]	RFPL [45]	47.0	61.0	74.6	86.8
	MoLo [42]	55.0	69.6	73.8	85.1
	D^2ST-Adapter	56.0	72.8	74.7	86.8
TRX [26]	RFPL [45]	44.6	64.6	66.2	87.3
	MoLo [42]	45.6	66.1	64.8	86.3
	D^2ST-Adapter	47.7	68.6	66.4	87.6
Bi-MHM [40]	HyRSM [40]	54.3	69.0	73.7	86.1
	MoLo [42]	56.6	70.6	74.0	85.6
	D^2ST-Adapter	57.0	73.6	75.0	87.0

configuring specialized sampling kernels for the spatial and temporal pathways.

Generalization across different matching metrics. To evaluate the generalization of our D^2ST -Adapter across different matching metrics, we conduct the experiments using three classical matching metrics on SSv2-Full and Kinetics, including OTAM [2], TRX [26], and Bi-MHM [40], and compare our model with the state-of-the-art methods corresponding to each metric. Table 5 presents the results, which show that our D^2ST -Adapter consistently outperforms other methods, especially on challenging SSv2-Full benchmark, validating the well generalization of the proposed D^2ST -Adapter across different matching metrics.

4.4. Visualization

In this section we visualize the shifted reference points learned by our D^2ST -Adapter to investigate the effectiveness of the proposed DSTA qualitatively. Following Deformable Attention [46], for each shifted reference point serving as key and value, we accumulate the attention

weights assigned by all queries as its relative importance. Then we visualize top-100 most important shifted reference points in each pathway for a video sample, as shown in Figure 5. Note that we sample 8 frames for all videos, if a reference point is shifted to a temporal position between two sampled frames, we visualize it on the nearest frame approximately for simplicity.

The results show that the shifted reference points learned by our model can always focus on the salient targets that are critical for action recognition in both the spatial and temporal pathways. Another interesting observation is that the shifted points in the spatial pathway are distributed densely in some specific frames to capture the spatial appearance features for the targets, while the shifted points in the temporal pathway are distributed uniformly among all frames to capture the temporal dynamic features. This is consistent with the design of specialized tailored DSTA modules for different pathways by configuring the sampling kernels accordingly.

5. Conclusion

We present D^2ST -Adapter, which is a novel adapter tuning method for few-shot action recognition. It is designed in dual-pathway architecture, which allows for disentangled encoding of spatial and temporal features. Moreover, we specially design the Deformable Spatio-Temporal Attention (DSTA) as the essential component of D^2ST -Adapter, which enables it to encode features in a global view while maintaining lightweight design. Extensive experiments demonstrate that our model compares favorably with other state-of-the-art methods, especially in the challenging scenarios involving complex temporal features.

Supplementary Material

A. Instantiation on ResNet-18 and ResNet-34

To investigate the performance of our D^2ST -Adapter on smaller backbones, we instantiate our model with ResNet-18 and ResNet-34 pre-trained on ImageNet, and conduct experiments to compare our model with other methods under the same experimental settings. The results in Table 8 show that our D^2ST -Adapter achieves the best performance using both backbones in all settings, which demonstrates the robustness of our method. While DSTA-Adapter, the convolutional version of our model, also performs well, it is still inferior to D^2ST -Adapter, which manifests the effectiveness of the proposed deformable spatio-temporal attention (DSTA).

B. Details of the Tuned Sampling Kernels

The sampling kernels of DSTA-S in the spatial pathway and DSTA-T in the temporal pathway of our D^2ST -Adapter can be tuned on a held-out validation set. Generally, DSTA-S should sample denser reference points in the spatial domain while DSTA-T samples more points in the temporal domain. For the instantiation of our model with ResNet, we configure the sampling kernel of DSTA in each convolutional stage individually since the feature maps in different convolutional stages may have different size. In contrast, we only need to tune one configuration for sampling kernel when using ViT as the backbone since the feature map always has fixed size in different stages. Table 6 shows the tuned configurations of the sampling kernels of DSTA-S and DSTA-T with different backbones. Besides, we also provide the configurations of sampling kernel for DSTA-Uniform module which is constructed to validate the effect of configuring the sampling kernel of DSTA in Table 4.

Table 6. Tuned sampling kernels (in the form of (T, H, W)) for DSTA-S in the spatial pathway and DSTA-T in the temporal pathway of our D^2ST -Adapter. Besides, the sampling kernel for DSTA-Uniform used in Table 4 for ablation study is also provided.

Backbone	Feature Map	Sampling Kernel in DSTA-S	Sampling Kernel in DSTA-T	Sampling Kernel in DSTA-Uniform
ResNet-50	(8, 56, 56)	(2, 8, 8)	(8, 4, 4)	(4, 4, 4)
ResNet-50	(8, 28, 28)	(2, 4, 4)	(8, 2, 2)	(4, 4, 4)
ResNet-50	(8, 14, 14)	(2, 4, 4)	(8, 2, 2)	(4, 4, 4)
ResNet-50	(8, 7, 7)	(2, 2, 2)	(8, 1, 1)	(4, 4, 4)
CLIP-ViT-B	(8, 14, 14)	(2, 4, 4)	(8, 2, 2)	(4, 4, 4)

C. Effect of the Inserted Position of D^2ST -Adapter

Theoretically, our D^2ST -Adapter can be inserted into any position of the backbone flexibly. To investigate the effect of the inserted position of D^2ST -Adapter on the perfor-

mance of the model, we conduct experiments with four different ways of inserting D^2ST -Adapters into the pre-trained CLIP-ViT-B backbone (comprising 12 learning stages) on SSv2-Small dataset: a) early-insertion, which inserts the D^2ST -Adapter into each of first 6 stages (close to the input), b) late-insertion that inserts the D^2ST -Adapter into each of last 6 stages (close to the output), c) skip-insertion, which inserts the adapter into the backbone every two stages and d) full-insertion that inserts the adapter into each learning stage.

As shown in Table 7, late-insertion, namely inserting the proposed D^2ST -Adapters into the last 6 stages, yields better performance than early-insertion, which implies that adapter tuning is more effective for task adaptation in deeper layers than in the shallower layers. It is reasonable since deeper layers generally capture the high-level semantic features, which are more relevant to task adaptation. Besides, full-insertion achieves the best performance at the expense of slightly more tunable parameters and memory usage.

Table 7. Effect of the inserted position of D^2ST -Adapter in CLIP-ViT-B on SSv2-Small dataset. Skip means adding D^2ST -Adapter every other stage.

Insertion Position	Tunable Parameters (%)	Memory Usage	1-shot	5-shot
Early-insertion	4.1%	15.5GB	48.4	64.6
Late-insertion	4.1%	15.2GB	54.2	68.5
Skip-insertion	4.1%	15.2GB	53.3	67.9
Full-insertion	7.9%	16.7GB	55.0	69.3

D. Effect of the Bottleneck Ratio of D^2ST -Adapter

The tunable parameter size is mainly determined by the bottleneck ratio of D^2ST -Adapter, defined as the ratio of down-sampled channel numbers to the initial size. Thus, we can balance between the model efficiency in terms of tunable parameter size and model effectiveness in terms of classification accuracy by tuning the bottleneck ratio. As shown in Table 9, larger bottleneck ratios typically yield more performance improvement while introducing more tunable parameters, and we set the bottleneck ratio to 0.25 in all the experiments based on the results.

E. More Visualizations

To provide more insight into the deformable spatio-temporal attention, we provide more visualization results in Figure 6. To be specific, we manually select a point within the salient object as the query token and visualize top-50 relevant shifted reference points to the query in terms of attention weights. The results show that our model is able to capture the salient object through the shifted reference points in both spatial and temporal domains.

Table 8. Performance of different methods using smaller backbones (*i.e.*, ResNet-18 and ResNet-34) on SSv2-Full dataset.

Method	ResNet-18					ResNet-34				
	1-shot	2-shot	3-shot	4-shot	5-shot	1-shot	2-shot	3-shot	4-shot	5-shot
OTAM [2]	39.4	45.0	46.6	47.4	49.0	40.6	45.2	48.0	48.9	49.2
TRX [26]	29.9	38.2	44.0	48.2	50.3	32.4	41.6	47.7	52.0	53.5
HyRSM [40]	46.6	54.7	58.7	60.7	61.1	50.0	57.5	61.9	63.3	64.8
MoLo [42]	<u>50.0</u>	<u>57.2</u>	61.6	<u>63.6</u>	64.6	<u>54.1</u>	<u>61.1</u>	<u>65.9</u>	<u>67.3</u>	<u>67.8</u>
ST-Adapter [25]	47.3	54.3	58.1	61.3	62.2	48.9	55.6	59.4	62.5	64.1
DST-Adapter (Ours)	<u>50.0</u>	56.9	<u>61.7</u>	63.4	<u>65.3</u>	52.1	59.3	63.4	65.8	67.5
D²ST-Adapter (Ours)	53.0	60.4	65.0	67.1	68.6	54.4	62.5	66.0	69.1	70.6

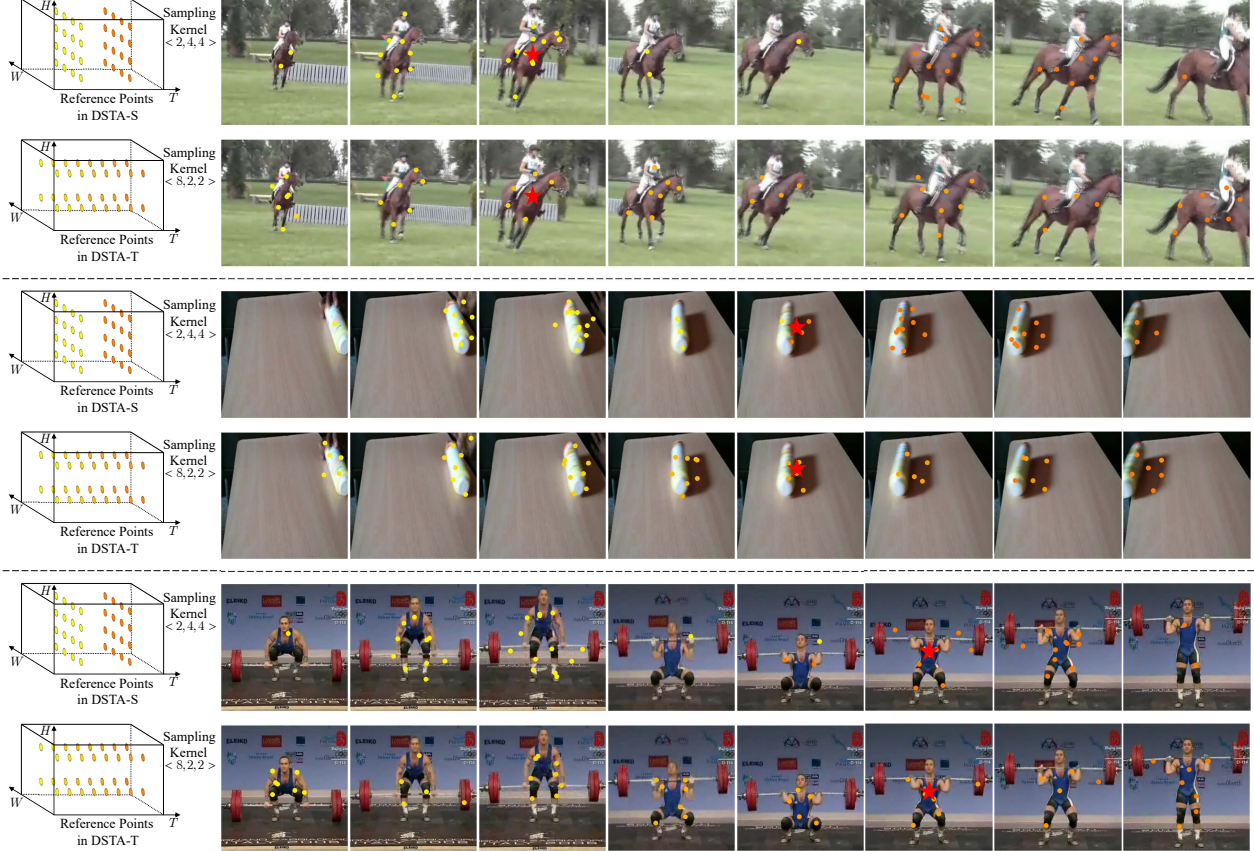


Figure 6. Given a selected query within the salient object, top-50 relevant shifted reference points in terms of attention weights in both pathways are visualized for three video samples. The red stars denote the selected query tokens while the circles denote relevant shifted reference points.

Table 9. Effect of the bottleneck ratio of D^2ST -Adapter in CLIP-ViT-B on SSv2-Small dataset.

Ratio	Tunable Parameters (%)	Memory Usage	1-shot	5-shot
0.0625	1.4%	15.2GB	53.4	68.1
0.125	3.2%	15.7GB	54.2	68.6
0.25	7.9%	16.7GB	55.0	69.3
0.5	20.2%	18.7GB	54.7	69.4

References

- [1] Mina Bishay, Georgios Zoumpourlis, and Ioannis Patras. TARN: Temporal attentive relation network for few-shot and zero-shot action recognition. In *BMVC*, 2019. 1, 3
- [2] Kaidi Cao, Jingwei Ji, Zhangjie Cao, Chien-Yi Chang, and Juan Carlos Niebles. Few-shot video classification via temporal alignment. In *CVPR*, pages 10618–10627, 2020. 1, 3, 5, 6, 7, 8, 10
- [3] Joao Carreira and Andrew Zisserman. Quo vadis, action recognition? a new model and the kinetics dataset. In *CVPR*,

- pages 6299–6308, 2017. 5
- [4] Shoufa Chen, Chongjian Ge, Zhan Tong, Jiangliu Wang, Yibing Song, Jue Wang, and Ping Luo. Adaptformer: Adapting vision transformers for scalable visual recognition. *NeurIPS*, 35:16664–16678, 2022. 2, 3
 - [5] Jia Deng, Wei Dong, Richard Socher, Li-Jia Li, Kai Li, and Li Fei-Fei. ImageNet: A large-scale hierarchical image database. In *CVPR*, pages 248–255, 2009. 5
 - [6] Carl Doersch, Ankush Gupta, and Andrew Zisserman. Crosstransformers: spatially-aware few-shot transfer. *NeurIPS*, 33:21981–21993, 2020. 2
 - [7] Alexey Dosovitskiy, Lucas Beyer, Alexander Kolesnikov, Dirk Weissenborn, Xiaohua Zhai, Thomas Unterthiner, Mostafa Dehghani, Matthias Minderer, Georg Heigold, Sylvain Gelly, et al. An image is worth 16x16 words: Transformers for image recognition at scale. In *ICLR*, 2021. 3, 5
 - [8] Christoph Feichtenhofer, Haoqi Fan, Jitendra Malik, and Kaiming He. SlowFast networks for video recognition. In *ICCV*, pages 6202–6211, 2019. 2, 4
 - [9] Chelsea Finn, Pieter Abbeel, and Sergey Levine. Model-agnostic meta-learning for fast adaptation of deep networks. In *ICML*, pages 1126–1135, 2017. 2
 - [10] Raghav Goyal, Samira Ebrahimi Kahou, Vincent Michalski, Joanna Materzynska, Susanne Westphal, Heuna Kim, Valentin Haenel, Ingo Fruend, Peter Yianilos, Moritz Mueller-Freitag, et al. The” something something” video database for learning and evaluating visual common sense. In *ICCV*, pages 5842–5850, 2017. 5
 - [11] Bharath Hariharan and Ross Girshick. Low-shot visual recognition by shrinking and hallucinating features. In *ICCV*, pages 3018–3027, 2017. 2
 - [12] Junxian He, Chunting Zhou, Xuezhe Ma, Taylor Berg-Kirkpatrick, and Graham Neubig. Towards a unified view of parameter-efficient transfer learning. In *ICLR*, 2021. 2, 3
 - [13] Kaiming He, Xiangyu Zhang, Shaoqing Ren, and Jian Sun. Deep residual learning for image recognition. In *CVPR*, pages 770–778, 2016. 1, 2, 3, 5
 - [14] Neil Houlsby, Andrei Giurgiu, Stanislaw Jastrzebski, Bruna Morrone, Quentin De Laroussilhe, Andrea Gesmundo, Mona Attariyan, and Sylvain Gelly. Parameter-efficient transfer learning for nlp. In *ICML*, pages 2790–2799, 2019. 2, 3, 7
 - [15] Yifei Huang, Lijin Yang, and Yoichi Sato. Compound prototype matching for few-shot action recognition. In *ECCV*, pages 351–368, 2022. 3, 6, 7
 - [16] Muhammad Abdullah Jamal and Guo-Jun Qi. Task agnostic meta-learning for few-shot learning. In *CVPR*, pages 11719–11727, 2019. 2
 - [17] Menglin Jia, Luming Tang, Bor-Chun Chen, Claire Cardie, Serge Belongie, Bharath Hariharan, and Ser-Nam Lim. Visual prompt tuning. In *ECCV*, pages 709–727, 2022. 2
 - [18] Diederik P Kingma and Jimmy Ba. Adam: A method for stochastic optimization. *arXiv preprint arXiv:1412.6980*, 2014. 5
 - [19] Hildegard Kuehne, Hueihan Jhuang, Estíbaliz Garrote, Tomaso Poggio, and Thomas Serre. HMDB: a large video database for human motion recognition. In *ICCV*, pages 2556–2563, 2011. 5
 - [20] Kai Li, Yulun Zhang, Kunpeng Li, and Yun Fu. Adversarial feature hallucination networks for few-shot learning. In *CVPR*, pages 13470–13479, 2020. 2
 - [21] Kunchang Li, Yali Wang, Peng Gao, Guanglu Song, Yu Liu, Hongsheng Li, and Yu Qiao. Uniformer: Unified transformer for efficient spatiotemporal representation learning. In *ICLR*, 2022. 4
 - [22] Shuyuan Li, Huabin Liu, Rui Qian, Yuxi Li, John See, Mengjuan Fei, Xiaoyuan Yu, and Weiyao Lin. TA2N: Two-stage action alignment network for few-shot action recognition. In *AAAI*, pages 1404–1411, 2022. 6, 7
 - [23] Meinard Müller. Dynamic time warping. *Information Retrieval for Music and Motion*, pages 69–84, 2007. 3
 - [24] Khoi D Nguyen, Quoc-Huy Tran, Khoi Nguyen, Binh-Son Hua, and Rang Nguyen. Inductive and transductive few-shot video classification via appearance and temporal alignments. In *ECCV*, pages 471–487, 2022. 3, 6, 7
 - [25] Juntong Pan, Ziyi Lin, Xiatian Zhu, Jing Shao, and Hongsheng Li. ST-Adapter: Parameter-efficient image-to-video transfer learning. In *NeurIPS*, 2022. 1, 2, 3, 6, 7, 10
 - [26] Toby Perrett, Alessandro Masullo, Tilo Burghardt, Majid Mirmehdi, and Dima Damen. Temporal-relational CrossTransformers for few-shot action recognition. In *CVPR*, pages 475–484, 2021. 1, 3, 5, 6, 7, 8, 10
 - [27] Alec Radford, Jong Wook Kim, Chris Hallacy, Aditya Ramesh, Gabriel Goh, Sandhini Agarwal, Girish Sastry, Amanda Askell, Pamela Mishkin, Jack Clark, et al. Learning transferable visual models from natural language supervision. In *ICML*, pages 8748–8763, 2021. 1, 2
 - [28] Sachin Ravi and Hugo Larochelle. Optimization as a model for few-shot learning. In *ICLR*, 2017. 2
 - [29] Karen Simonyan and Andrew Zisserman. Two-stream convolutional networks for action recognition in videos. *NeurIPS*, 27, 2014. 2
 - [30] Jake Snell, Kevin Swersky, and Richard Zemel. Prototypical networks for few-shot learning. *NeurIPS*, 30, 2017. 2, 3
 - [31] Khuram Soomro, Amir Roshan Zamir, and Mubarak Shah. UCF101: A dataset of 101 human actions classes from videos in the wild. *arXiv preprint arXiv:1212.0402*, 2012. 5
 - [32] Flood Sung, Yongxin Yang, Li Zhang, Tao Xiang, Philip HS Torr, and Timothy M Hospedales. Learning to compare: Relation network for few-shot learning. In *CVPR*, pages 1199–1208, 2018. 2
 - [33] Yi-Lin Sung, Jaemin Cho, and Mohit Bansal. Lst: Ladder side-tuning for parameter and memory efficient transfer learning. *NeurIPS*, 35:12991–13005, 2022. 3
 - [34] Anirudh Thatipelli, Sanath Narayan, Salman Khan, Rao Muhammad Anwer, Fahad Shahbaz Khan, and Bernard Ghanem. Spatio-temporal relation modeling for few-shot action recognition. In *CVPR*, pages 19958–19967, 2022. 2, 6, 7
 - [35] Du Tran, Lubomir Bourdev, Rob Fergus, Lorenzo Torresani, and Manohar Paluri. Learning spatiotemporal features with 3d convolutional networks. In *ICCV*, pages 4489–4497, 2015. 1

- [36] Du Tran, Heng Wang, Lorenzo Torresani, Jamie Ray, Yann LeCun, and Manohar Paluri. A closer look at spatiotemporal convolutions for action recognition. In *CVPR*, pages 6450–6459, 2018. 4
- [37] Oriol Vinyals, Charles Blundell, Timothy Lillicrap, Daan Wierstra, et al. Matching networks for one shot learning. *NeurIPS*, 29, 2016. 2, 3
- [38] Limin Wang, Yuanjun Xiong, Zhe Wang, Yu Qiao, Dahua Lin, Xiaoou Tang, and Luc Van Gool. Temporal segment networks: Towards good practices for deep action recognition. In *ECCV*, pages 20–36, 2016. 2
- [39] Ruizhe Wang, Duyu Tang, Nan Duan, Zhongyu Wei, Xuan-Jing Huang, Jianshu Ji, Guihong Cao, Daxin Jiang, and Ming Zhou. K-adapter: Infusing knowledge into pre-trained models with adapters. In *ACL*, pages 1405–1418, 2021. 2, 3
- [40] Xiang Wang, Shiwei Zhang, Zhiwu Qing, Mingqian Tang, Zhengrong Zuo, Changxin Gao, Rong Jin, and Nong Sang. Hybrid relation guided set matching for few-shot action recognition. In *CVPR*, pages 19948–19957, 2022. 1, 2, 3, 5, 6, 7, 8, 10
- [41] Xiang Wang, Shiwei Zhang, Jun Cen, Changxin Gao, Yingya Zhang, Deli Zhao, and Nong Sang. Clip-guided prototype modulating for few-shot action recognition. *arXiv preprint arXiv:2303.02982*, 2023. 1, 5, 6, 7
- [42] Xiang Wang, Shiwei Zhang, Zhiwu Qing, Changxin Gao, Yingya Zhang, Deli Zhao, and Nong Sang. Molo: Motion-augmented long-short contrastive learning for few-shot action recognition. In *CVPR*, pages 18011–18021, 2023. 1, 2, 3, 5, 6, 7, 8, 10
- [43] Yu-Xiong Wang, Ross Girshick, Martial Hebert, and Bharath Hariharan. Low-shot learning from imaginary data. In *CVPR*, pages 7278–7286, 2018. 2
- [44] Jiamin Wu, Tianzhu Zhang, Zhe Zhang, Feng Wu, and Yongdong Zhang. Motion-modulated temporal fragment alignment network for few-shot action recognition. In *CVPR*, pages 9151–9160, 2022. 2, 3, 6, 7
- [45] Haifeng Xia, Kai Li, Martin Renqiang Min, and Zhengming Ding. Few-shot video classification via representation fusion and promotion learning. In *ICCV*, pages 19311–19320, 2023. 2, 8
- [46] Zhuofan Xia, Xuran Pan, Shiji Song, Li Erran Li, and Gao Huang. Vision transformer with deformable attention. In *CVPR*, pages 4794–4803, 2022. 2, 4, 8
- [47] Jiazheng Xing, Mengmeng Wang, Yong Liu, and Boyu Mu. Revisiting the spatial and temporal modeling for few-shot action recognition. In *AAAI*, pages 3001–3009, 2023. 6, 7
- [48] Jiazheng Xing, Mengmeng Wang, Yudi Ruan, Bofan Chen, Yaowei Guo, Boyu Mu, Guang Dai, Jingdong Wang, and Yong Liu. Boosting few-shot action recognition with graph-guided hybrid matching. In *ICCV*, pages 1740–1750, 2023. 2, 6, 7
- [49] Taojiannan Yang, Yi Zhu, Yusheng Xie, Aston Zhang, Chen Chen, and Mu Li. AIM: Adapting image models for efficient video action recognition. In *ICLR*, 2022. 3
- [50] Han-Jia Ye, Hexiang Hu, De-Chuan Zhan, and Fei Sha. Few-shot learning via embedding adaptation with set-to-set functions. In *CVPR*, pages 8808–8817, 2020. 2
- [51] Sung Whan Yoon, Jun Seo, and Jaekyun Moon. TAPNet: Neural network augmented with task-adaptive projection for few-shot learning. In *ICML*, pages 7115–7123, 2019. 2
- [52] Hongguang Zhang, Li Zhang, Xiaojuan Qi, Hongdong Li, Philip HS Torr, and Piotr Koniusz. Few-shot action recognition with permutation-invariant attention. In *ECCV*, pages 525–542, 2020. 1, 2, 5
- [53] Ruixiang Zhang, Tong Che, Zoubin Ghahramani, Yoshua Bengio, and Yangqiu Song. MetaGAN: An adversarial approach to few-shot learning. *NeurIPS*, 31, 2018. 2
- [54] Songyang Zhang, Jiale Zhou, and Xuming He. Learning implicit temporal alignment for few-shot video classification. In *IJCAI*, 2021. 2, 6, 7
- [55] Sipeng Zheng, Shizhe Chen, and Qin Jin. Few-shot action recognition with hierarchical matching and contrastive learning. In *ECCV*, pages 297–313, 2022. 3, 6, 7
- [56] Kaiyang Zhou, Jingkang Yang, Chen Change Loy, and Ziwei Liu. Learning to prompt for vision-language models. *IJCV*, 130(9):2337–2348, 2022. 2
- [57] Linchao Zhu and Yi Yang. Compound memory networks for few-shot video classification. In *ECCV*, pages 751–766, 2018. 2, 5, 6, 7
- [58] Linchao Zhu and Yi Yang. Label independent memory for semi-supervised few-shot video classification. *IEEE TPAMI*, 44(1):273–285, 2020. 2, 6, 7